Geophysical Research Letters

Correspondence to:
J. F. Lübbecke,
jluebbecke@geomar.de

Stand-Alone Eastern Pacific Coastal Warming Events

Joke F. Lübbecke[1,2] [iD], **Daniel Rudloff[1,2], and Lothar Stramma[1]** [iD]

[1]GEOMAR Helmholtz Centre for Ocean Research Kiel, Kiel, Germany, [2]Faculty of Mathematics and Natural Sciences, Christian-Albrechts-Universität zu Kiel, Kiel, Germany

Abstract A pronounced warm anomaly occurred at the Peruvian coast in early 2017. This "Coastal Niño" caused heavy rainfalls, leading to flooding in Peru and Ecuador. At the same time, neutral conditions prevailed in the equatorial Pacific. Using observational sea surface temperature data sets and an ocean reanalysis product for the time period 1900 to 2010, previous similar events are investigated. Eighteen coastal warming events without corresponding equatorial Pacific warming are identified. Further analysis shows, however, that only four of these events are not connected to the central equatorial Pacific. All other periods of strong coastal warm anomalies are directly followed or preceded by El Niño-like conditions. The "stand-alone" coastal warming events are characterized by comparatively low equatorial heat content. We thus hypothesize that the depleted heat content in the equatorial Pacific in the wake of the strong 2015/2016 El Niño prevented the warming to spread westward in 2017.

Plain Language Summary Warmer than normal sea surface temperatures (SSTs) in the southeastern tropical Pacific off the South American coast can lead to anomalously heavy rainfalls over Peru. These SST anomalies are typically linked to El Niño events in the equatorial Pacific Ocean, but there are some events, such as in early 2017, that occur independently of El Niño. In this study, we seek to identify how often such "stand-alone" coastal warming events take place and what distinguishes them from events that are connected to El Niño. Analyzing different products that provide long time series of SST, we find that only very few events are really not preceded or followed by basin-scale warm anomalies in the central and eastern equatorial Pacific. These events are characterized by low heat content, that is, a discharged state, in the equatorial Pacific.

1. Introduction

In February to April 2017 extremely warm sea surface temperatures (SST) were observed in the far eastern tropical Pacific off Peru and Ecuador, accompanied by heavy rainfalls and flooding over land. The impact on the Peruvian ecosystem and society was comparable to the strong El Niño events of 1982/1983 and 1997/1998 (Ramírez & Briones, 2017; Rodríguez-Morata et al., 2019). Due to its serious impacts, the pronounced warming received a lot of media attention under the term "Coastal El Niño."

A peculiar feature of this event was that it was not connected to a warming in the central equatorial Pacific, which was actually in a weak La Niña state for the fall and early winter of 2016 according to the classification of the National Oceanic and Atmospheric Administration (NOAA) Climate Prediction Center (http://origin.cpc.ncep.noaa.gov/products/analysis_monitoring/ensostuff/ONI_v5.php; Echevin et al., 2018). Studies that have investigated the origin of the coastal SST anomaly agree on the important role of anomalous northerly coastal winds (Echevin et al., 2018; Garreaud, 2018; Peng et al., 2019; Rodríguez-Morata et al., 2019). This weakening of the local southeasterly trade winds has in turn been traced back to a weakening of the free tropospheric westerlies impinging the subtropical Andes (Garreaud, 2018) and an anomalous weakening of the middle-upper level subtropical westerly flow (Rodríguez-Morata et al., 2019). The role of equatorial ocean dynamics for the onset of the 2017 coastal warming is a little more controversial. While Rodríguez-Morata et al. (2019) and Hu et al. (2019) conclude from the absence of a clear Kelvin wave propagation signal in the thermocline depth anomalies from the Tropical Atmosphere Ocean/Triangle Trans-Ocean Buoy Network (TAO/TRITON) moored buoy array in the tropical Pacific (Figure 1) that equatorial waves were not the dominant forcing mechanism, Echevin et al. (2018) and Peng et al. (2019) find a contribution of downwelling Kelvin and coastally trapped waves to the development of the warm anomaly in their model experiments and observed sea level anomalies.
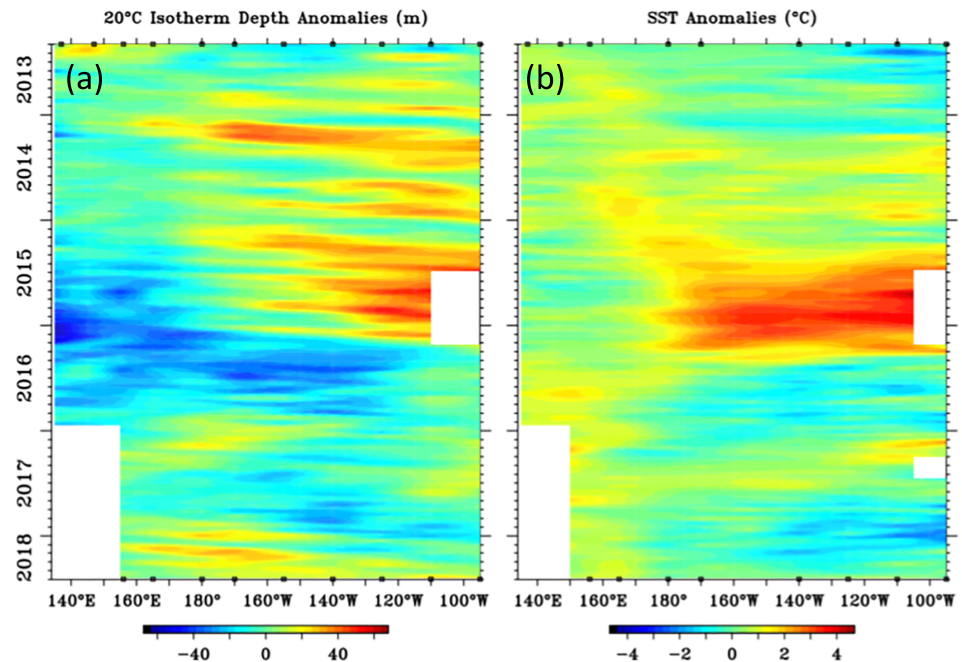
Figure 1. Longitude-time diagram of (a) thermocline (20 °C isotherm) depth anomalies in m and (b) SST anomalies in degrees Celsius averaged over 2°S to 2°N from the TAO/TRITON (obtained from https://www.pmel.noaa.gov/tao/drupal/disdel/). SST = sea surface temperature.

To highlight the differences to classical El Niño events, Ormaza-González and Cedeño (2017) suggested to call the 2017 event a "Carneval coastal warming" or "rapid coastal warming event." Following their suggestion, we will here avoid the term "Niño" and instead refer to "coastal warming events." A coastal warming event occurring in 1925 has been described in detail by Takahashi and Martínez (2017). In a recent study, Hu et al. (2019) have investigated the coastal warming events since 1979. Of the seven events they detected, they found that only 2008 was similar to 2017 in terms of mechanisms while the other coastal warming periods either followed basin-scale El Niños or were forced by downwelling Kelvin waves that resulted from westerly wind bursts in the western Pacific, that is, a classical El Niño forcing mechanism.

In the present study, we extend the time period, going back to 1900, to address the question whether there have been more stand-alone coastal warming events similar to 2017 and offer a hypothesis on what sets these events apart from other coastal warming events.

2. Data and Methods

Monthly SST data for the time period 1900 to 2010 were taken from HadISST (Rayner et al., 2003), the COBE SST2 data set (Ishii et al., 2005) at a horizontal resolution of 1°, and the NOAA ERSSTv5 data set (Huang et al., 2017) at 2° horizontal resolution, all provided by the NOAA/OAR/ESRL/PSD, Boulder, Colorado, USA. For subsurface ocean variables as well as wind stress and SST we use the "historical" simulation from the Simple Ocean Data Assimilation (SODA) reanalysis product (SODA2.2.4; Carton & Giese, 2008) for the time period 1900 to 2010. SODA2.2.4 is forced with 20CRv2 surface winds (Compo et al., 2011) and has 40 vertical levels and a horizontal resolution of 0.5°. We have calculated interannual anomalies by subtracting a repeated mean seasonal cycle based on the time period 1981 to 2010 as well as the linear trend of the time series. Further, a 1.1- to 5-year band-pass filter has been applied to the time series to filter out decadal modulations that differ slightly between the SST products.

To identify coastal warming events, we use the filtered SST anomalies for the time period 1900 to 2010 averaged over the Niño1 + 2 (80°W to 90°W, 0°N to 10°S) and Niño3.4 (120°W to 170°W, 5°S to 5°N) regions (Figures S1 and S2 in the supporting information). If the SST anomaly exceeds 0.6 times the standard deviation of the time series in the Niño1 + 2 region while it is below the standard deviation of the time series in the

Niño3.4 region and the difference between the two regions is greater than 0.45 °C in at least three out of four SST data sets for at least two consecutive months, we classify this event as a coastal warming (Figure S3 and Table S1). This definition is chosen to exclude SST anomalies that are just the coastal extension of an El Niño event taking place in the central equatorial Pacific. Hu et al. (2019) dealt with this by subtracting the Nino3.4 related variability from the Nino1 + 2 index and defining thresholds for both the regular and the El Niño–Southern Oscillation-adjusted Nino1 + 2 indices that had to be exceeded for three consecutive overlapping seasons. As will be discussed below, most but not all of the years identified as coastal warming events agree between both methods.

Using our definition, the following 18 years show up as coastal warming events: 1902, 1923, 1925, 1932, 1943, 1945, 1951, 1953, 1957, 1965, 1969, 1972, 1976, 1979, 1983, 1993, 1998, and 2008. Almost all of them peak in the austral fall and winter months, that is, between April and August (Table S1). For the overlapping time period of 1979 to 2008, the events of 1983, 1998, and 2008 agree with the classification of Hu et al. (2019). Our method did not identify a coastal warming event in any of the data sets in 1987 while Hu et al. (2019) did not define an event in 1993. The index time series in Hu et al. (2019, their Figure 5) shows that the anomaly in 1987 is considerably reduced when adjusting for Nino3.4-related variability but still passes their threshold, while the warm event in 1993 is visible but does not exceed the threshold for the required duration.

Equatorial warm water volume (WWV) has been computed as the water volume above the 20 °C isotherm in the equatorial region. This has been done by linearly interpolating the subsurface temperatures from SODA2.2.4 on a grid with a 5-m vertical resolution for each grid point. The shallowest depth with temperatures below 20 °C is then used as the depth of the isotherm (z20). To obtain the WWV, the depth of the 20 °C isotherm is averaged along the equator (2.25°S to 2.25°N, 140.25°E to 75.25°W) and multiplied by the area.

3. Results

3.1. SST Evolution of Coastal Warming Events

A special feature of the 2017 coastal warming event was that the central to eastern equatorial Pacific stayed relatively cool; that is, the coastal warming was neither directly preceded nor followed by an El Niño event (Echevin et al., 2018). Looking at the development of the coastal warming events defined above, we see that —consistent with the findings of Hu et al. (2019)—the coastal warmings of 1983 and 1998 occurred in the aftermath of the two biggest El Niño events of the late twentieth century. Contrary to the canonical decay phase described by Harrison and Larkin (1998), SSTs at the South American coast stayed warm for several months after conditions went back to normal in the central equatorial Pacific in both of these years. As discussed by Hu et al. (2019) the decaying phase of the strong El Niño events in 1982/1983 and 1997/1998 involved the development of an equatorially centered intertropical convergence zone, leading to westerly wind anomalies and thus the persistence of warm SST anomalies at the South American coast (Lengaigne & Vecchi, 2010). These events were thus very different from what happened in 2017.

For most of the other years that meet our definition of coastal warming events (1902, 1923, 1925, 1951, 1953, 1957, 1965, 1972, and 1976), we find that they tend to extend into the central equatorial Pacific within the following 6 months, that is, develop into a regular El Niño event or at least a warm equatorial anomaly. All of them are actually listed as El Niño years in a study by Yu and Kim (2013), which determines different types of El Niño events by means of pattern correlation. The evolution toward a warm equatorial Pacific is illustrated by composites of SST anomalies centered on the month of the maximum SST anomaly in the Nino1 + 2 region (Figure 2a). It has long been recognized that some El Niño events start from a coastal warming and propagate westward (e.g., Rasmusson & Carpenter, 1982), and it is this connection to the Peruvian coast that actually gave the El Niño phenomenon its name.

It is interesting to note that the 1925 coastal warming event, as one of the few "coastal Niños" described in the literature (Takahashi & Martínez, 2017), falls into this category. In their detailed study of this event, Takahashi and Martínez (2017) actually describe the evolution from the initial coastal warming into the 1925/1926 El Niño. Due to this connection to the central equatorial Pacific it is here regarded differently from the 2017 coastal warming. Differences in the forcing mechanisms will be discussed in the following subsections.
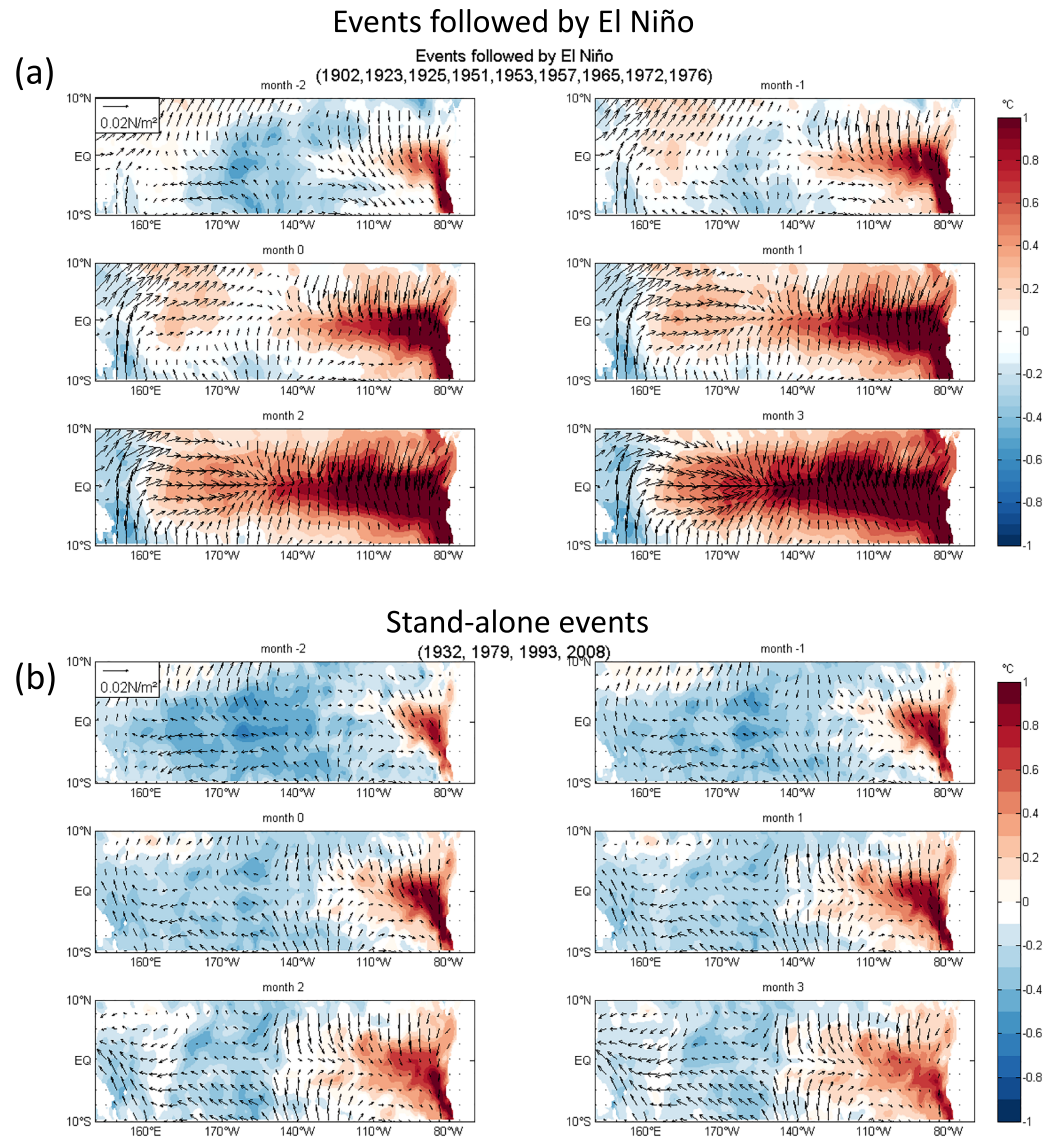
AGU
100
ADVANCING EARTH
AND SPACE SCIENCE

Geophysical Research Letters

10.1029/2019GL084479

Figure 2. SST and wind stress evolution of coastal warming events from two months prior to 3 months after the peak SST anomaly from Simple Ocean Data Assimilation 2.2.4: composite of (a) events followed by El Niño and (b) stand-alone coastal warming events. SST = sea surface temperature.

Focusing on the remaining seven events we find that also the warm anomalies in 1943 and 1945 extended quite far from the coast into the Pacific basin, so that they cannot be regarded as pure coastal events. For 1969, the SST difference between the coastal and equatorial Pacific was the result of a brief cooling episode in the central Pacific during a general warm phase (Figure S3). This year is actually also listed as an El Niño year by Yu and Kim (2013). This leaves only four events that are similar to 2017 in that they are neither followed nor preceded by warm SSTs in the central equatorial Pacific, namely, 1932, 1979, 1993, and 2008. Interestingly, just like the coastal warming in 2017 that occurred a little more than one year after the big El Niño of 2015/2016, all of these events were preceded by El Niños with a lag of a bit over 1 year (Yu & Kim, 2013; Figure S3). A composite of the four "stand-alone" coastal warming events is shown in Figure 2 b. For those events and the ones followed by El Niño we will look at the local wind forcing, remote forcing by equatorial waves and the role of equatorial heat content in the next sections.

3.2. Local Wind Forcing

The prevailing southerly winds along the Peruvian coast are climatologically weakest from February to April. During all coastal warming events defined above, northerly anomalies, corresponding to a
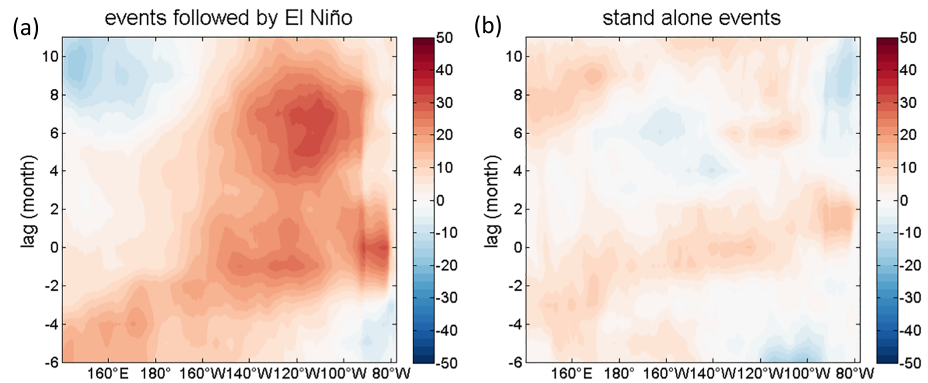
Figure 3. Composites of thermocline depth (depth of the 20 °C isotherm, z20) anomalies in meters from Simple Ocean Data Assimilation 2.2.4 for (a) coastal warming events followed by El Niño and (b) stand-alone coastal warming events.

weakening or—in the cases of 1925 and 1976—even a reversal of the alongshore winds occurred at the onset of the event, in particular to the north of the warm SST anomaly (Figure 2). Such a weakening of the winds typically leads to reduced coastal upwelling, which is driven by the alongshore winds, and less latent heat loss, and would thus contribute to a warming of the region, consistent with the mechanisms described by Garreaud (2018), Hu et al. (2019), and Peng et al. (2019) for the 2017 event. In particular, the 1925 coastal SST anomaly has been shown to be related to strong northerly winds (Takahashi & Martínez, 2017). Echevin et al. (2018) also addressed the role of wind stress curl changes in the 2017 event and found an important contribution from a deepening of the thermocline and onshore geostrophic current anomalies. The combined effect of reduced upwelling, heat flux anomalies, and anomalous geostrophic currents in response to weakened alongshore winds and associated wind stress curl anomalies have also recently been discussed with respect to a coastal warm anomaly in the southeastern tropical Atlantic Ocean (Lübbecke et al., 2019). In addition to local processes, remote forcing from the equatorial region can play an important role in generating SST anomalies along the Peruvian coast by deepening the thermocline as a result of Kelvin wave propagation. This process will be looked at in the next section.

3.3. Remote Forcing From the Equatorial Pacific

At the onset of El Niño events, downwelling Kelvin waves propagate eastward along the equator, deepening the thermocline. They can continue along the South American coast as coastal Kelvin waves (Colas et al., 2008; Enfield et al., 1987), expressed as a depression of the thermocline and the associated subsurface warming that can lead to warm surface temperatures through reduced upwelling and mixing of cooler subsurface waters. We here use z20 from SODA2.2.4 as a measure of the thermocline depth to detect those Kelvin waves.

For the coastal warming events followed by El Niño defined above, equatorial Kelvin wave propagation is visible from a longitude-time diagram of z20 along the equator, starting from about 6 to 4 months before the peak of the event (Figure 3a). The time at which the Kelvin wave reaches the eastern Pacific coincides with the beginning of the coastal warming, suggesting that the associated subsurface warming was indeed important for their onset. A pronounced deepening of the thermocline is obvious in the eastern equatorial Pacific for the months following the coastal warming, matching the timing of the equatorial SST anomaly. In contrast to the study by Takahashi and Martínez (2017) the signature of a downwelling Kelvin wave is also clearly visible in spring 1925 in thermocline depth anomalies from SODA reanalysis.

The stand-alone coastal warming events on the other hand are only associated with a very weak thermocline anomaly that propagates along the equator (Figure 3b), suggesting that equatorial wave dynamics are less important for the development of these events. However, there might be some contribution from downwelling Kelvin and coastally trapped waves. For 2017, some studies argue that they actually played a significant role in the onset of the event (Echevin et al., 2018; Peng et al., 2019).
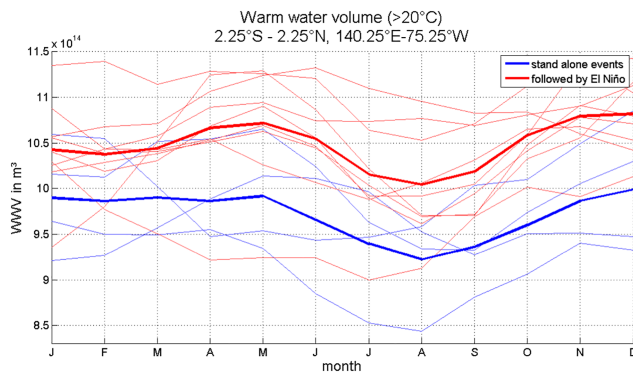
Figure 4. Equatorial Pacific warm water volume >20 °C (WWV; in 10^{14} m^3) for events followed by an El Niño event (red lines, thick line shows average) and stand-alone coastal warming events (blue lines, thick line shows average).

3.4. Equatorial Heat Content

Consistent with the findings by Hu et al. (2019) our results indicate that the occurrence of strong warm anomalies at the Peruvian coast only very rarely happens independently of El Niño in the equatorial Pacific. An interesting indication as to why these events do not spread into the central equatorial Pacific is given by the equatorial heat content. One prerequisite for El Niño events is the buildup of high heat content in the equatorial band (e.g., Meinen & McPhaden, 2000). Comparing the coastal warming events that were followed by an equatorial warming with the stand-alone events, we find comparatively high WWV in the preceding boreal winter for the first category but low WWV for the stand-alone events (Figure 4). The coastal warming event of 2017 also took place during a phase of low equatorial heat content following the 2015/16 El Niño (Figure S4; see also Timmermann et al., 2018, their Figure 2).

As mentioned above, all stand-alone events including 2017 were preceded by El Niño events with a lag of about a year, that is, occurred in a phase in which equatorial heat content is typically depleted (e.g., Meinen & McPhaden, 2000; Timmermann et al., 2018) in accordance with recharge oscillator theory (Jin, 1997). Our results thus suggest that coastal warming events cannot spread into the central equatorial Pacific when they occur in years in which the equatorial heat content is anomalously low.

4. Summary and Discussion

In an analysis of direct SST observations and the reanalysis product SODA2.2.4 we identified 18 coastal warming events that took place between 1900 and 2010 at the Peruvian coast with no simultaneous warm anomalies in the central equatorial Pacific, that is, events reminiscent of the strong 2017 Coastal Niño. While some of them develop as early in the year as February/March, the majority of these events take place between April and August, which has probably limited their impact on rainfall over land. We find that in contrast to 2017 most of the events do have a connection to the central equatorial Pacific and are either preceded or followed by an El Niño in the same year. Only four events, 1932, 1979, 1993, and 2008, are stand-alone coastal warming events, similar to 2017.

For the coastal warming events that were followed by warm conditions in the central equatorial Pacific, both local wind and remote equatorial forcing appear to have played a role in generating the SST anomalies. Notably all of those events occurred before the Pacific climate shift in 1976/1977 (Miller et al., 1994). This is consistent with the findings by Wang (1995) who reported a shift in the onset region of El Niño from the South American coast to the eastern central Pacific in the late 1970s and linked this to the changes in the background state of the tropical Pacific. These events thus appear to follow the mechanisms for westward propagating SST anomalies that have been described for canonical El Niños before the climate shift. These mechanisms involve a strong zonal advective feedback and westward zonal mean currents (Santoso et al., 2013) as well as a westward propagating Rossby wave reflected from the Kelvin wave that initiates the warming at the Peruvian coast (Dewitte & Takahashi, 2019). Also, the previously described 1925 event, which was found to be mainly locally forced and associated with severe rainfall in Peru and Ecuador belongs to this category as it developed into a basin-wide El Niño (Takahashi & Martínez, 2017).

As for the forcing of the stand-alone events, local wind forcing appears to be dominant with a weaker contribution for equatorial and coastally trapped waves. The northerly and westerly wind anomalies have been associated with a sustained weakening of the free tropospheric westerly flow impinging the Andes (Garreaud, 2018), an anomalous seasonal change in the intertropical convergence zone and trade winds in the eastern equatorial Pacific (Hu et al., 2019), and atmospheric teleconnections between the western and far eastern Pacific (Echevin et al., 2018). On intraseasonal time scales, Dewitte et al. (2011) also discussed the role of the South Pacific anticyclone and the Madden-Julian Oscillation in driving upwelling anomalies off Peru. In order to forecast coastal warming events, it will be important to get a detailed understanding of the large-scale atmospheric conditions that can lead to the local wind anomalies.

Differences in equatorial heat content point to the important role of the equatorial Pacific background state for determining whether an initial coastal warming event can spread into the central equatorial Pacific. Notably all stand-alone events occurred after an El Niño event with a lag of about one year, indicating the importance of the depleted heat content in the discharged phase following an El Niño. Consistent with recharge-discharge oscillator theory, during this phase the equatorial Pacific is not susceptible to the development of an El Niño. The low equatorial heat content in the wake of the strong 2015/2016 El Niño might in particular have prevented the warming to spread into the central equatorial Pacific in 2017.

References

Carton, J., & Giese, B. S. (2008). A reanalysis of ocean climate using Simple Ocean Data Assimilation (SODA). *Monthly Weather Review*, *136*, 2999–3017. https://doi.org/10.1175/2007MWR1978.1

Colas, F., Capet, X., McWilliams, J. C., & Shchepetkin, A. (2008). 1997–98 El Niño off Peru: A numerical study. *Progress in Oceanography*, *79*, 138–155. https://doi.org/10.1016/j.pocean.2008.10.015

Compo, G. P., Whitaker, J. S., Sardeshmukh, P. D., Matsui, N., Allan, R. J., Yin, X., et al. (2011). The twentieth century reanalysis project. *Quarterly Journal of the Royal Meteorological Society*, *137*(654), 1–28. https://doi.org/10.1002/qj.776

Dewitte, B., Illig, S., Renault, L., Goubanova, K., Takahashi, K., Gushchina, D., et al. (2011). Modes of covariability between sea surface temperature and wind stress intraseasonal anomalies along the coast of Peru from satellite observations (2000–2008). *Journal of Geophysical Research*, *116*, C04028. https://doi.org/10.1029/2010JC006495

Dewitte, B., & Takahashi, K. (2019). Diversity of moderate El Niño events evolution: Role of air-sea interactions in the eastern tropical Pacific. *Climate Dynamics*, *52*, 7455–7476. https://doi.org/10.1007/s00382-017-4051-9

Echevin, V., Colas, F., Espinoza-Morriberon, D., Vasquez, L., Anculle, T., & Gutierrez, D. (2018). Forcings and evolution of the 2017 Coastal El Niño off Northern Peru and Ecuador. *Frontiers in Marine Science*, *5*, 367. https://doi.org/10.3389/fmars.2018.00367

Enfield, D. B., Cornejo-Rodriguez, M. P., Smith, R. L., & Newberger, P. A. (1987). The equatorial source of propagating variability along the Peru coast during the 1982–1983 El Niño. *Journal of Geophysical Research*, *92*, 14,335–14,346. https://doi.org/10.1029/JC092iC13p14335

Garreaud, R. D. (2018). A plausible trigger for the 2017 coastal El Niño. *International Journal of Climatology*, *38*(S1), e1296–e1302. https://doi.org/10.1002/joc.5426

Harrison, D. E., & Larkin, N. K. (1998). El Niño–Southern Oscillation sea surface temperature and wind anomalies, 1946 to 1993. *Reviews of Geophysics*, *36*(3), 353–399. https://doi.org/10.1029/98RG00715

Hu, Z.-Z., Huang, B., Zhu, J., Kumar, A., & McPhaden, M. J. (2019). On the variety of coastal El Niño events. *Climate Dynamics*, *52*(12), 7537–7552. https://doi.org/10.1007/s00382-018-4290-4

Huang, B., Thorne, P. W., Banzon, V. F., Boyer, T., Chepurin, G., Lawrimore, J. H., et al. (2017). Extended Reconstructed Sea Surface Temperature version 5 (ERSSTv5), Upgrades, validations, and intercomparisons. *Journal of Climate*, *30*(20), 8179–8205. https://doi.org/10.1175/JCLI-D-16-0836.1

Ishii, M., Shouji, A., Sugimoto, S., & Matsumoto, T. (2005). Objective analyses of sea-surface temperature and marine meteorological variables for the 20th century using ICOADS and the Kobe Collection. *International Journal of Climatology*, *25*, 865–879. https://doi.org/10.1002/joc.1169

Jin, F.-F. (1997). An equatorial ocean recharge paradigm for ENSO. Part I: Conceptual model. *Journal of the Atmospheric Sciences*, *54*, 811–829. https://doi.org/10.1175/1520-0469(1997)054%3C0811:AEORPF%3E2.0.CO;2

Lengaigne, M., & Vecchi, G. A. (2010). Contrasting the termination of moderate and extreme El Niño events in coupled general circulation models. *Climate Dynamics*, *35*, 299–313. https://doi.org/10.1007/s00382-009-0562-3

Lübbecke, J. F., Brandt, P., Dengler, M., Kopte, R., Lüdke, J., Richter, I., et al. (2019). Causes and evolution of the southeastern tropical Atlantic warm event in early 2016. *Climate Dynamics*, *53*(1-2), 261–274. https://doi.org/10.1007/s00382-018-4582-8

Meinen, C. S., & McPhaden, M. J. (2000). Observations of warm water volume changes in the equatorial Pacific and their relationship to El Niño and La Niña. *Journal of Climate*, *13*, 3551–3559. https://doi.org/10.1175/1520-0442(2000)013%3C3551:OOWWVC%3E2.0.CO;2

Miller, A. J., Cayan, D. R., Barnett, T. P., Graham, N. E., & Oberhuber, J. M. (1994). The 1976–77 climate shift of the Pacific Ocean. *Oceanography*, *7*(1), 21–26. https://www.jstor.org/stable/43925525

Ormaza-González, F. I., & Cedeño, J. (2017). Coastal El Niño 2017 or simply: The carnival coastal warming event? *MOJ Ecology & Environmental Science*, *2*(8). https://doi.org/10.15406/mojes.2017.02.00054

Peng, Q., Xie, S.-P., Wang, D., Zheng, X.-T., & Zhang, H. (2019). Coupled ocean-atmosphere dynamics of the 2017 extreme coastal Niño. *Nature Communications*, *10*(1), 298. https://doi.org/10.1038/s41467-018-08258-8

Ramírez, I. J., & Briones, F. (2017). Understanding the El Niño Costero of 2017: The definition problem and challenges of climate forecasting and disaster responses. *International Journal of Disaster Risk*, *8*(4), 489–492. https://doi.org/10.1007/s13753-017-0151-8

Rasmusson, E. M., & Carpenter, T. H. (1982). Variations in tropical sea surface temperature and surface wind fields associated with the Southern Oscillation/El Niño. *Monthly Weather Review*, *110*, 354–384. https://doi.org/10.1175/1520-0493(1982)110%3C0354:VITSST%3E2.0.CO;2

Rayner, N. A., Parker, D. E., Horton, E. B., Folland, C. B., Alexander, L. V., Rowell, D. P., et al. (2003). Global analyses of sea surface temperature, sea ice, and night marine air temperature since the late nineteenth century. *Journal of Geophysical Research*, *108*(D14), 4407. https://doi.org/10.1029/2002JD002670

Rodríguez-Morata, C., Díaz, H. F., Ballesteros-Canovas, J. A., Rohrer, M., & Stoffel, M. (2019). The anomalous 2017 coastal El Niño event in Peru. *Climate Dynamics*, *52*(9-10), 5605–5622. https://doi.org/10.1007/s00382-018-4466-y

Santoso, A., McGregor, S., Jin, F. F., Cai, W., England, M. H., An, S. I., et al. (2013). Late-twentieth-century emerge of the El Niño propagation asymmetry and future projections. *Nature*, *504*(7478), 126–130. https://doi.org/10.1038/nature12683

Takahashi, K., & Martínez, A. G. (2017). The very strong coastal El Niño in 1925 in the far-eastern Pacific. *Climate Dynamics*, *52*(12), 7389–7415. https://doi.org/10.1007/s00382-017-3702-1

Timmermann, A., An, S.-I., Kug, J.-S., Jin, F.-F., Cai, W., Capotondi, A., et al. (2018). El Niño–Southern Oscillation complexity. *Nature*, *559* (7715), 535–545. https://doi.org/10.1038/s41586-018-0252-6

Wang, B. (1995). Interdecadal changes in El Niño onset in the last four decades. *Journal of Climate*, *8*(2), 267–285. https://doi.org/10.1175/1520-0442(1995)008%3C0267:ICIENO%3E2.0.CO;2

Yu, J.-Y., & Kim, S. T. (2013). Identifying the types of major El Niño events since 1870. *International Journal of Climatology*, *33*, 2105–2112. https://doi.org/10.1002/joc.3575